Optics and Spectroscopy, Vol. 92, No. 3, 2002, pp. 395–401. Translated from Optika i Spektroskopiya, Vol. 92, No. 3, 2002, pp. 438–444.

SOLID STATE SPECTROSCOPY

Resonance Raman Scattering by Excitonic Polaritons in $CuGaS_2$

N. N. Syrbu*, M. Blazhe*, I. M. Tiginyanu*, and V. E. Tezlevan**

**Technical University of Moldova, Chisinau, MD-2012 Moldova*

***Institute of Applied Physics, Academy of Sciences of Moldova, Chisinau, MD-2028 Moldova*

Received January 30, 2001; in final form, October 8, 2001

Abstract—Resonance Raman scattering by exciton polaritons in crystals of $CuGaS_2$ under excitation with the 4880 and 4765 Å lines of an Ar^+ laser at 9 K is studied. Lines of one- and two-phonon scattering of excitonic polaritons are found and studied. It is shown that the 1LO and 2LO phonons are arranged in accordance with their energies as the Stokes shifts move farther away from the excitation energy. *© 2002 MAIK "Nauka/Interperiodica".*

INTRODUCTION

Polaritonic effects play an important role in the formation of low-temperature emission, absorption, and reflection spectra near the exciton resonances [1]. The basic features of the polariton luminescence in the II–VI crystals and some other two-component materials have been studied in detail [2–6]. Study of the resonance Raman scattering and hot luminescence of excitonic polaritons in multicomponent materials has just started. Papers [7–9] discuss the first experimental data on Raman scattering with energies of the *S* state of *A* exciton series in $CuGaS_2$ crystals. These studies consider a great number of one-phonon and multiphonon Raman scattering lines. No emission lines of excitonic polaritons were found. In [10], the allowed Γ_4 ($\mathbf{E} \parallel c$) and Γ_5 ($\mathbf{E} \perp c$) and forbidden Γ_3 ($\mathbf{E} \parallel c$, $\mathbf{E} \perp c$) excitons are analyzed. For multicomponent materials, it is important to determine the contribution of vibrational modes of various symmetries in the polariton luminescence. When studying the resonance scattering of the excitonic polaritons in the $CuGaS_2$ crystal with the symmetry D_{2d}^{12}, it is of interest whether its six phonons of *E* symmetry and phonons of B_2 and B_1 symmetry are aligned in accordance with their energies. The $n = 1$ lines of *A* and *B* excitons in this crystal are spaced apart by a much larger energy gap (120 meV) than in CdS (15 meV). Because of this, the thermalized luminescence in the $CuGaS_2$ crystals has almost no effect on the resonance multiphonon radiation.

In this paper, we analyze the experimental spectra of resonance scattering in $CuGaS_2$ crystals at 9 K and reveal the lines of one- and two-phonon scattering. New data on the energy alignment of phonons in the spectra of excitonic polariton scattering are also reported.

EXPERIMENTAL

As samples, we used $CuGaS_2$ crystals with dimensions of $10 \times 8 \times 4$ mm and reflecting faces, grown by the gas-transport method. The dimensions and quality of the natural faces allowed reliable measurement of the reflection, luminescence, and Raman spectra from the same area of the crystal. The specular face of some crystals was parallel to the *c* axis.

The spectra were recorded by a setup based on a DFS-32 double Raman spectrometer. The spectral width of the spectrometer slit was 0.015 Å when measuring the reflection and about 0.05–0.1 Å when recording the luminescence and Raman spectra.

The samples were mounted on the cold holder of a closed helium cryogenic system "LTS-22 C 330 Workhorse-type Optical System," so that the sample temperature was 9.0 ± 0.5 K. The resonance Raman scattering was excited by the 4880 and 4765 Å lines of an Ar laser with the power no higher than 100 mW in the illuminated spot about 1 mm in diameter. The reflection and absorption of the samples were studied with the continuous spectrum of an incandescent lamp (~100 W).

RESULTS AND DISCUSSION

The spectra of reflection from the $CuGaS_2$ crystal mirror face were measured in the $\mathbf{E} \parallel c$ polarization. The reflection spectra (Fig. 1) show a structure characteristic of excitons, with the $n = 1$, 2, and 3 lines of the 3 Γ_4 exciton.

The transmission spectra of the samples with the thickness $d \cong 2$–3.5 μm were measured in the region of the exciton reflection ($n = 1$) in the $\mathbf{E} \parallel c$ polarization (Fig. 1, curve *K*). As can be seen, the minimum of the transmission spectrum (the absorption coefficient is 4730 cm^{-1}) is close to the reflection spectrum peak at 2.50109 eV.

0030-400X/02/9203-0395$22.00

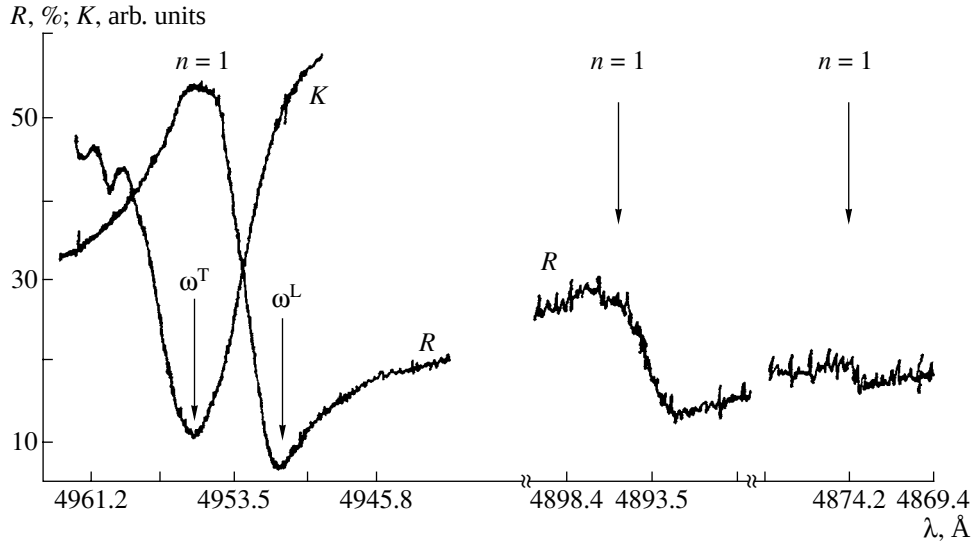

Fig. 1. (*R*) Reflection and (*K*) absorption spectra of $CuGaS_2$ crystals at 9 K in the region of $n = 1, 2, 3$ of the *A*-excitonic series. The absorption is measured in the $\mathbf{E} \parallel c$ polarization in the samples about two–three μm thick; lines of $n = 2$ and 3 are recorded using the widened spectrometer slit.

In the short-wavelength spectral region, the reflection spectra show the $n = 2$ line at 2.5332 eV and a poorly pronounced feature at 2.5428 eV ($n = 3$). From the spectrum, we determined the Rydberg constant of excitons, $R = 0.03247$ eV, and the band gap, $E_g^{n=\infty} = 2.54135$ eV. To determine the exciton state parameters, we analyzed the reflection band in the 4942–4960 Å region. The best fit to the experimental data is attained using the Hapfield–Thomas model of the exciton reflection with the Pekar additional boundary conditions. The reflection contours are calculated by the method reported elsewhere [11–16].

The reflection spectra calculations yield the following main parameters of the exciton resonance for $n = 1$ of the Γ_4 exciton in $CuGaS_2$: the resonance energy $\hbar\omega_0 = 2.5011$ eV, the longitudinal-transverse splitting $\hbar\omega_{LT} \cong 4.1$ meV ($\hbar\omega_{LT}$ varies from 3.9 to 4.4 meV for different samples), the exciton translation mass $M = 2m_0$ (m_0 is the free electron mass), the "dead" (exciton-free) layer thickness $l = 11$ Å, the decay $\hbar\Gamma = 0.6$ meV, and the background dielectric constant $E_{zz} = 7$. Thus, the decay factor in the $CuGaS_2$ crystal is shown to be $\gamma < \omega_{LT}$.

Figure 2 shows the Raman spectra measured in the backward configuration $[x(zz)\bar{x}]$ under the excitation by the 4765-Å line of the Ar^+ laser. An intense peak related to the upper branch polaritons, $\omega^L_{n_1}$, is observed around 2.504 eV (Figs. 2, 3). Near the reflection peak and the transmission minimum, we observe the scattering peak related to the lower branch polaritons, $\omega^T_{n_1}$ (Figs. 2, 3). On the short-wavelength side of $\omega^L_{n_1}$, we observe the e_1–e_{11} Raman scattering lines (Fig. 2), and the e_{11} peak can be seen on the long-wavelength side of the $\omega^T_{n_1}$. Farther to the long-wavelength side from the e_{12} line, the luminescence of the bound excitons occurs, which will be discussed in our next paper. Thus, when exciting $CuGaS_2$ crystals by the 4765 Å line of an Ar^+ laser, we observe the e_1–e_{11} scattering lines caused by the two-phonon resonance Raman scattering by excitonic polaritons and the scattering lines of the upper and lower branches of excitonic polaritons, $\omega^L_{n_1}$ and $\omega^T_{n_1}$ (Figs. 2, 3). The e_1 line, shifted by 535.6 cm^{-1} from the 4765-Å laser line, is related to the scattering with two phonons, $E^6_{LO} + E^3_{LO}$; the e_2 line is caused by $E^3_{LO} + B^3_{2LO}$ scattering, the e_3 line corresponds to the $A_1 + E^4_{LO}$ phonons, etc. (see Table 1). The frequencies and symmetries of phonons in the $CuGaS_2$ crystal are taken from papers [17–20].

All the e_1–e_{10} lines are satisfactorily explained by the relaxation of the excitonic polaritons with two phonons involved, while the e_{11} line is apparently caused by three-phonon scattering.

Thus, under excitation of $CuGaS_2$ crystals by the 4765-Å line of the Ar^+ laser, the resonance scattering of excitonic polaritons occurs with the participation of 2LO phonons of different symmetry. Table 1 gives the energies, Stokes shifts, and peak intensities of the scattering lines, as well as the combinations of 2LO phonons involved in the scattering. As can be seen from Fig. 2, the half-width of the 2LO phonon lines is somewhat smaller than the half-widths of the $\omega^L_{n_1}$ and $\omega^T_{n_1}$

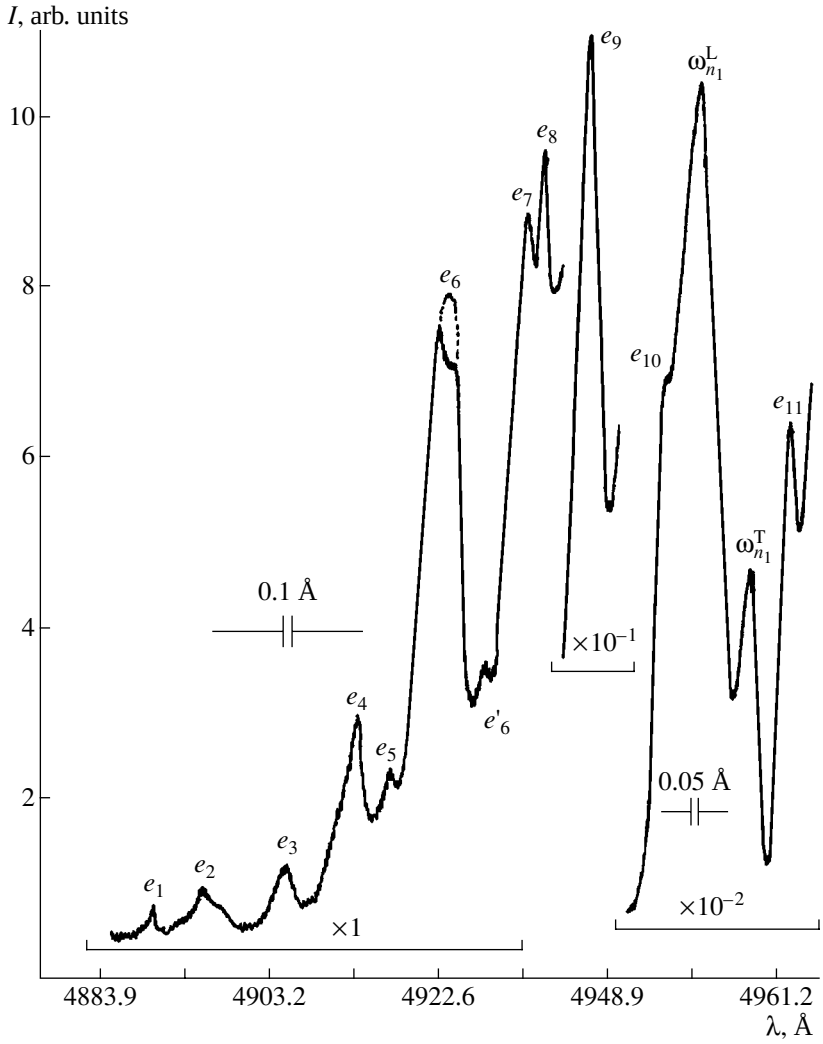

Fig. 2. Resonance scattering of excitonic polaritons in $CuGaS_2$ crystals in the $x(zz)\bar{x}$ configuration at 9 K under the excitation by the Ar^+ laser with $\lambda = 4765$ Å.

lines. A similar relation is observed for the resonance Raman scattering by 1LO phonons (see Fig. 4, Table 2). The intensity of the scattering by 1LO phonons is lower than by 2LO phonons by a factor of 3–5.

As the exciting wavelength changes from 4765 to 4880 Å, the energies of all the phonon lines change, while the peaks corresponding to excitonic polaritons, $\omega^{L}_{n_1}$ and $\omega^{T}_{n_1}$, retain the same energies. These variations in the line energies are quite understandable since different phonons and phonon combinations participate in the 1LO and 2LO processes. At the same time, the stable energy of the 2.5040 eV peak proves our assumption that this line is related to the upper polariton branch rather than to the three-phonon process, as was assumed in [7]. We also believe that the α peak at 2.502 eV [7] corresponds to the peak we observed at 2.5011 eV ($\omega^{T}_{n_1}$) and is caused by the lower polariton branch.

The scattering lines are more intense, the closer they lie to the $\omega^{L}_{n_1}$ and $\omega^{T}_{n_1}$ lines, which is true both for 2LO (Table 1) and 1LO scattering (Table 2). Evidently, the occupancy of the "hot" levels increases closer to the exciton band bottom [3]. The intensity of the scattering excited by 4765-Å radiation is almost an order of magnitude higher than the scattering under 4880-Å excitation. This dependence is also observed in CdS and ZnTe crystals [4–6], where the intensity of the 2LO scattering exceeds that of 1LO scattering. It is also noteworthy that the $\omega^{T}_{n_1}$ line is more intense than the $\omega^{L}_{n_1}$ line when excited by the 4880-Å radiation, while under the 4765-Å excitation we observe the inverse relation.

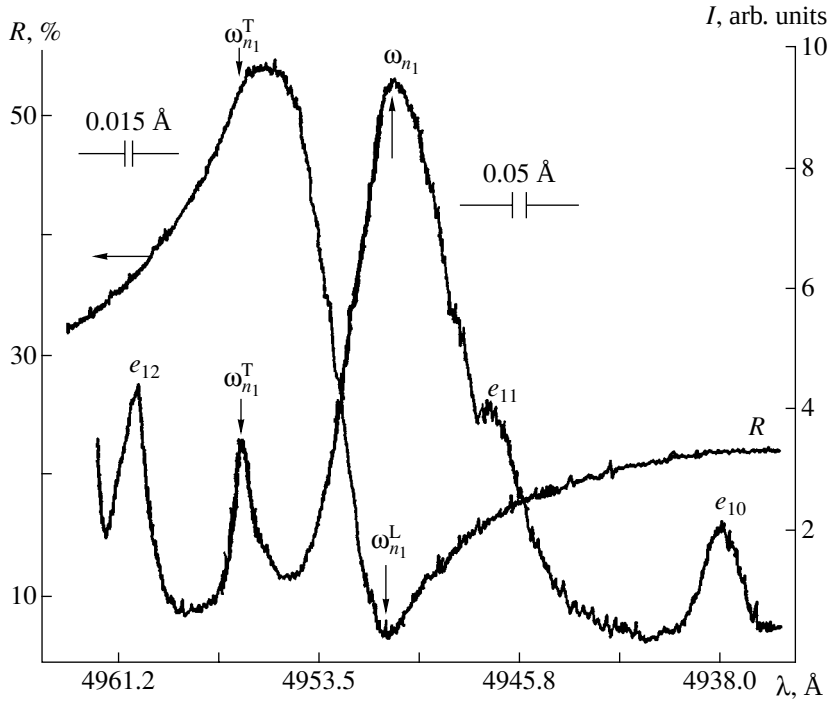

Fig. 3. Spectra of the reflection in the **E** || *c* polarization and of Raman scattering in $CuGaS_2$ crystals in the $x(zz)\bar{x}$ configuration at 9 K under the 4765-Å excitation.

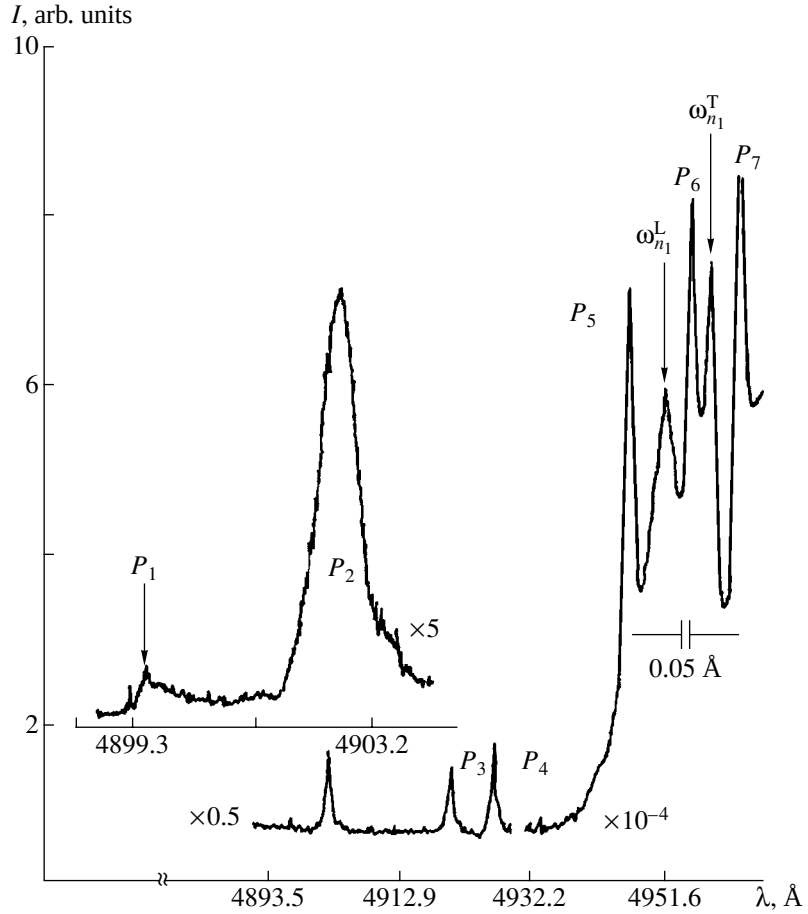

Fig. 4. The resonance Raman spectra in the region of excitonic polaritons in the $x(zz)\bar{x}$ configuration (backscattering) under the 4880-Å excitation by an Ar^+ laser.

Table 1. Parameters of the two-phonon resonance Raman scattering in the region of excitonic polaritons in $CuGaS_2$ at 9 K under the excitation by the Ar^+ laser line with $\lambda = 4765$ Å

Line	Energy position, eV	Stokes shift, cm^{-1}	Peak intensity, arb. units	Possible combinations of phonons responsible for the Stokes shift	Symmetry of the phonons
e_1	2.5352	535.6		367 + 167	$E^6_{LO} + E^3_{LO}$
e_2	2.5322	559.8		167 + 392.8	$E^3_{LO} + B^3_{2LO}$
e_3	2.5277	569.1		312 + 284	$A_1 + E^4_{LO}$
e_4	2.5238	627.6		345 + 284	$E^5_{LO} + E^4_{LO}$
e_5	2.5188	667.9	5	392.8 + 273	$B^3_{2LO} + E^4_{LO}$
e_6	2.5163	688	15	286.3 + 401	$B^2_{2LO} + B^3_1$
e_7	2.5139	707.5	19	312 + 392.8	$A_1 + B^3_{2LO}$
e_8	2.5131	713.9	23	347 + 367.2	$E^5_{LO} + E^6_{LO}$
e_9	2.5102	737.3	35	347 + 392.8	$E^5_{LO} + B^3_{2LO}$
e_{10}	2.5060	771.2	130	367 + 401	$E^6_{LO} + B^3_1$
ω^L_{n1}	2.5040		180		
ω^T_{n1}	2.5011	830	110		Three-phonon
e_{11}	2.4987		125		

Table 2. Parameters of the one-phonon resonance Raman scattering in the region of $CuGaS_2$ excitonic polaritons at 9 K under the excitation by the Ar^+ laser line $\lambda = 4880$ Å

Line	Line energy, eV	Stokes shift, cm^{-1}	Peak intensity, arb. units	Half-width, cm^{-1}	Symmetry of the vibrational modes responsible for the scattering
P_1	2.5298	84.7	0.2		E^1_{LO}
P_2	2.5285	95.2	5		B^1_{2LO}
P_3	2.5194	167.8	3	1.9	E^3_{LO}
P_4	2.5163	194	4	3.9	E^3_{LO} or B^2_1
P_5	2.5065	272.6	4.8	4.7	E^4_{LO} or B^2_{2TO}
P_6	2.5021	308.2	140	3.9	A_1
P_7	2.4982	339.6	250	3.9	E^5_{LO}
$\omega^L_{n_1}$	2.5040		40	12	
$\omega^T_{n_1}$	2.5011		96	5	

Hence, at the 4880-Å excitation the scattering occurs by the lower polariton branch, and the upper polariton branch plays the main part in the scattering excited by the 4765-Å line.

At the excitation of the $CuGaS_2$ crystals by the Ar^+ laser line $\lambda = 4880$ Å, the Raman spectra in the $x(zz)\bar{x}$ configuration at 9 K show the peaks P_1–P_7 and $\omega^L_{n_1}$ and

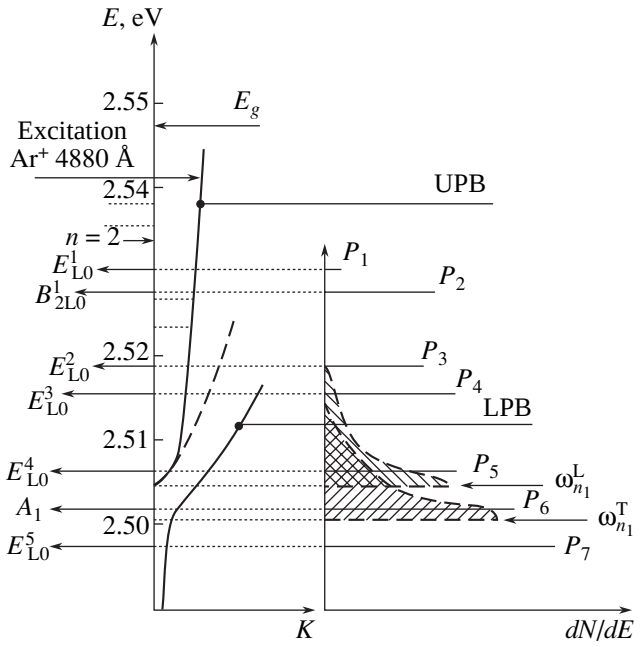

Fig. 5. Schematic representation of the cascade relaxation of excitonic polaritons in $CuGaS_2$ at 1LO phonons of various symmetries at 9 K under the 4880-Å excitation by an Ar^+ laser.

$\omega^T_{n_1}$. The excitation energy, $\hbar\omega_i$ = 2.5403 eV, is lower than the continuum energy E_g = 2.5474 eV, and is somewhat higher than the energy of the state n = 2 (2.5356 eV) for the $CuGaS_2$ crystal. This results in the resonance excitation of excitonic polaritons and in the one-phonon resonance Raman scattering in the region of excitonic polaritons (Fig. 4).

When the $CuGaS_2$ crystals are excited by a radiation with a wavelength within the fundamental absorption region (λ = 4880 Å), the excitation efficiently decays with the participation of LO phonons, which leads to the formation of free excitons with different intrinsic or kinetic energies. The scattering line energy E_R differs from the excitation-quantum energy by the LO phonon energy and is equal to

$$E_R = E_i - E_{LOj},$$

where j defines the order of the phonon participation in the scattering. This means that, in the course of the excitation-energy relaxation, the phonons are arranged in accordance to their energies (Table 2). The line P_1 is related to the vibrational mode E^1_{LO}, the line P_2 is caused by the mode B^1_{2LO}, the line P_3 corresponds to the mode B^1_{2LO}, etc. (Fig. 4, Table 1). To identify the phonon energies and symmetries, we used the data given in [14]. However, the relaxation of energy of the "hot" excitons considerably changes near the band bottom, as it occurs in CdS and other II–VI compounds [3, 5, 6]. In the $CuGaS_2$ crystals, different phonons participate in the 1LO and 2LO relaxation.

As can be seen from Fig. 4 and Table 2, the P_5, P_6, and P_7 lines are more intense than the P_1–P_4 lines. The lines P_5, P_6, and P_7 have higher intensity than the lines of the excitonic polaritons of the upper ($\omega^L_{n_1}$) and the lower ($\omega^T_{n_1}$) branches. An increase in the Raman line intensity closer to the excitonic resonance is observed almost in all the II–VI compounds. In addition, the scattering by two, three, and more phonons is more intense than the one-phonon scattering [3, 15, 16, 21].

Thus, the LO phonons of various symmetries are dominant in the $CuGaS_2$ scattering spectra. As the excitation wavelength changes from 4880 to 4765 Å, the $\omega^T_{n_1}$ becomes more intense, and the $\omega^L_{n_1}$ line weakens. This indicates that the population density of the lower polariton branch decreases at the two-phonon scattering. In the case of the excitation at λ = 4765 Å, the LO phonon scattering occurs via the upper polariton branch, and its population density exceeds that of the lower polariton branch. Table 2 presents the Stokes shift; the peak intensity; and the half-widths of P_1–P_7, $\omega^L_{n_1}$ and $\omega^T_{n_1}$ lines, as well as symmetries of the one-phonon vibrational modes responsible for the relaxation of the excitonic polaritons.

The scheme of the cascade relaxation of the excitonic polaritons by the LO phonons of various symmetry at 9 K for the 4880-Å excitation is shown in Fig. 5. The central part shows the schematic of the upper and lower polariton branches n = 1 (UPB_{n_1} and LPB_{n_1}) and the positions of n = 2 and E_g. The right-hand section illustrates the nonequilibrium population of the exciton band, dN/dE, and the relative intensity of the scattering lines. A schematic of the one-phonon scattering at the LO phonons of various symmetries is shown to the left. For convenience, the polariton dispersion law $E(\mathbf{k})$ is given in one direction of the wave vector $\mathbf{k}$.

CONCLUSIONS

The above experiments proved that the basic mechanisms of the resonant scattering of excitonic polaritons in the multicomponent crystal $CuGaS_2$ are similar to the II–VI compounds (CdS, CdTe, ZnTe, etc.). At the same time, it is shown that at the Stokes scattering the LO and 2LO phonons (six phonons of E symmetry and phonons of B_1 and B_2 symmetries) are arranged in accordance with their energies. The half-widths of the one- and two-phonon Raman scattering lines are found to be narrower than those of the upper and lower branches of excitonic polaritons. The intensity of the one-phonon scattering intensity is lower than that of the two-phonon scattering by a factor of 3–5.

REFERENCES

1. V. M. Agranovich and V. L. Ginzburg, *Crystal Optics with Spatial Dispersion and Excitons* (Nauka, Moscow, 1979; Springer-Verlag, New York, 1984), Chap. III.
2. *Light Scattering in Solids III*, Ed. by M. Cordona and G. Gunthrerodt (Springer-Verlag, Berlin, 1982).
3. S. A. Permogorov, Author's Abstract of Doctoral Dissertation (Leningrad, 1981).
4. B. Bendow, *Polariton Theory of Resonance Raman Scattering in Solids* (Springer-Verlag, Berlin, 1978); Springer Tracts Mod. Phys. **82**, 89 (1978).
5. S. A. Permogorov, Phys. Status Solidi B **68**, 9 (1975); *Exitons*, Ed. by M. Sturge, E. Rashba, *et al.* (North-Holland, Amsterdam, 1982).
6. S. A. Permogorov and V. Travnikov, Solid State Commun. **29**, 615 (1979).
7. N. Tsuboi, H. Uchiki, H. Jshikawa, and S. Iida, Jpn. J. Appl. Phys., Suppl. **32**, 584 (1993).
8. N. Tsuboi, H. Uchici, M. Sawada, *et al.*, Physica B (Amsterdam) **185**, 348 (1993).
9. M. Susaki, N. Yamomoto, B. Prevot, and C. Schwab, Jpn. J. Appl. Phys. **35**, 1652 (1996).
10. M. Susaki, K. Wakita, and N. Yamomoto, Jpn. J. Appl. Phys., Part 1 **38**, 2787 (1999).
11. S. A. Permogorov and V. V. Travnikov, Fiz. Tverd. Tela (Leningrad) **13**, 709 (1971) [Sov. Phys. Solid State **13**, 586 (1971)].
12. S. A. Permogorov and A. V. Sel'kin, Fiz. Tverd. Tela (Leningrad) **15**, 3025 (1973) [Sov. Phys. Solid State **15**, 2015 (1973)].
13. E. L. Ivchenko and A. V. Sel'kin, Zh. Éksp. Teor. Fiz. **76**, 1837 (1979) [Sov. Phys. JETP **49**, 933 (1979)].
14. S. A. Permogorov, A. V. Sel'kin, and V. V. Travnikov, Fiz. Tverd. Tela (Leningrad) **15**, 1822 (1973) [Sov. Phys. Solid State **15**, 1215 (1973)].
15. S. A. Permogorov, V. V. Travnikov, and A. V. Sel'kin, Fiz. Tverd. Tela (Leningrad) **14**, 3642 (1972) [Sov. Phys. Solid State **14**, 3051 (1972)].
16. S. Permogorov and V. Travnikov, Phys. Status Solidi B **78**, 389 (1976).
17. G. Carlone, D. Olego, A. Jayaraman, and M. Cardona, Phys. Rev. B **22**, 3877 (1980).
18. M. Bettini and W. B. Holzaptel, Solid State Commun. **16**, 17 (1975).
19. J. P. van der Ziel, A. E. Meixner, H. M. Kasper, and I. A. Ditzenberger, Phys. Rev. B **60**, 4286 (1974).
20. W. H. Koschel and M. Bettini, Phys. Status Solidi B **72**, 729 (1975).
21. A. Nakamura and C. Weisbuch, Solid State Commun. **32**, 301 (1979).

Translated by M. Basieva